Improving the Nomad microscopic walker model

Mario Campanella*. Serge Hoogendoorn*
Winnie Daamen*

**Transport & Planning Department, Delft University of Technology, Delft, the Netherlands, (Tel: 0031-15-2784914; e-mail: m.c.campanella@ tudelft.nl)*

Abstract: This paper presents the results of two calibration efforts and improvements of the Nomad microscopic walker model. Each calibration consisted in comparing the outcome of 19 sets of model parameters with results from laboratory experiments. Three different flows were used in the calibrations: bidirectional, unidirectional and a narrow bottleneck. For the first two types of flow the macroscopic speed-density relation is used for comparison. For the narrow-bottleneck the capacity for the bottleneck is assessed. Additionally, quantitative measures of self-organizing lane formation for the bidirectional flow are included in the calibration. In the first calibration effort only 4 parameter sets did not present gridlocks in the bidirectional flow and their results are presented. These four sets over estimated the capacity of the bottleneck and the efficiency of the unidirectional flows. These results are discussed and it is shown that a modification in the model is necessary. A modified model is presented and submitted to a new round of calibration. One parameter set showed significant improvement for the speed-density relations and the capacity of the bottleneck. The experience gained in this calibration effort indicates that pedestrian microscopic models can be calibrated over several types of flows simultaneously. However, this research shows that care must be taken when using only macroscopic flow properties for calibration. They may not guarantee the generality of the model due to the complexity and variety of possible flows.

Keywords: Pedestrian microscopic model, calibration, Nomad pedestrian model, social force models.

1. INTRODUCTION

Microscopic traffic models are modelled over high dimension spaces and usually present a large set of parameters. Calibrating a microscopic model is a difficult task and one of the goals is to achieve a general prediction capability Brockfeld *et al.*, 2004. For pedestrian models this problem is exacerbated by the fact that there is an uncountable diversity of possible flows and population composition.

The usual method of calibrating microscopic pedestrian models is by comparing relations between density, speed and flow (so-called fundamental diagrams) to those obtained empirically (Seyfried and Schadschneider, 2008; Buchmueller and Weidmann, 2006; Klüpfel, 2005). Most reports on calibration of microscopic pedestrian models focus in few aggregated aspects of the flows (Asano *et al.*, 2007; Berrou *et al.*, 2005) and generally do not show results for different types of flows. A different approach of parameter estimation was proposed by (Hoogendoorn *et al.*, 2005) using trajectory data of real life experiments. They estimated model parameters for individual pedestrians and used the sample to discuss inter-pedestrian differences and derive parameter correlations in the population on multiple flows.

1.1 Self-organisation

Self organizing phenomena occur in many traffic systems. In particularly in pedestrian flows several kinds are observed, such as lane formation in bidirectional flows, formation of diagonal stripes in crossing flows and zipper-effects in bottlenecks. What these phenomena have in common is the appearance of spatial patterns characterized by a specific distribution of individuals over the walking area (Hoogendoorn and Daamen, 2005; Helbing *et al.*, 2005). In bidirectional flows pedestrians tend to walk in the same direction in dynamically formed lanes. In crossing flows, clusters of pedestrians walking in the same direction display patterns resembling diagonal stripes.

Since pedestrian behaviour is characterised by self-organisation phenomena, the calibration of microscopic pedestrian simulation models has to consider the reproduction of these phenomena among other things. The majority of the microscopic simulation models claim to reproduce the most important self organizing phenomena (Teknomo, 2006; Pelechano *et al.*, 2007). However, there is not much evidence indicating that microscopic simulation models have been calibrated on self-organisation phenomena quantitatively.

1.2 Paper outline

This paper presents a calibration process for the Nomad pedestrian microscopic simulation model combining the fit of speed-density fundamental diagrams, capacity of narrow corridors and a quantitative measure of self-organizing lane formation. First, the basic Nomad walker model is presented in section 2. In section 3, the empirical results obtained in laboratory experiments are presented in the form of speed-density diagrams for two types of pedestrian flows: unidirectional and bidirectional. The experimental data of the bidirectional flow is also used to extract a distribution of the number of lanes. A narrow bottleneck is used to calculate averaged capacity. An equivalent simulation set-up has been created and twenty six parameter sets for the Nomad pedestrian model have been investigated (section 4). The investigation compares speed-density relations for the bidirectional, unidirectional flows, capacity for the narrow-bottleneck and lane distribution for a set of parameters. The results for the basic model are discussed (section 5). A modification of the Nomad model is presented (section 6) and calibrated again (section 7). The section 7 ends with a discussion about the new results and the quality of the predictions of the modified model. In the conclusion we outline some conclusions about this calibration effort.

2. NOMAD WALKER MODEL

Nomad is a microscopic pedestrian simulation tool developed by the department of Transport & Planning of the Delft University of Technology. The tool is implemented using a model proposed by (Hoogendoorn and Bovy, 2003). The model describes all actions of the pedestrians as activities and is based on the micro-economic notion of subjective utility maximization.

The walker model describes the walking behaviour of pedestrians. Pedestrians are described as compressible (circular) particles. Let $\vec{x}_p(t)$, $\vec{v}_p(t)$ and $\vec{a}_p(t)$ respectively denote the location, the velocity and the acceleration of pedestrians. The walker model is described as follows:

$$\frac{d\vec{x}_p(t)}{dt} = \vec{v}_p(t) \tag{1}$$

$$\frac{d\vec{v}_p(t)}{dt} = \vec{a}_p(t) \tag{2}$$

The acceleration is assumed to be a linear addition of different factors affecting pedestrian walking behaviour, namely the desire to stay as close as possible to a desired trajectory leading as direct as possible to the pedestrian's destination $\vec{s}_p(t)$, the avoidance of other pedestrians $\vec{r}_p(t)$, the avoidance of obstacles $\vec{o}_p(t)$, the contact forces that arise when pedestrians are colliding $\vec{p}_p(t)$ and a stochastic noise $\vec{\varepsilon}_p(t)$ accounting for the population heterogeneity and unrepresented factors. The acceleration model for the basic Nomad model is described in (3):

$$\vec{a}_p(t) = \vec{s}_p(t) + \vec{r}_p(t) + \vec{o}_p(t) + \vec{p}_p(t) + \vec{\varepsilon}_p(t) \tag{3}$$

Where:

$$\vec{s}_p(t) = \frac{\vec{v}_p^0(t) - \vec{v}_p(t)}{\mathrm{T}_p} \tag{4}$$

$\vec{v}_p^0(t)$ Desired velocity of pedestrian p

T_p Relaxation time of pedestrian p

The desired speed $\vec{v}_p^0(t)$ is a vector tangent to the desired trajectory with length equal to the free speed of pedestrian p. The model assumes free speeds to be normally distributed with variance s^0.

$$\vec{r}_p(t) = -A_p^0 \sum_{q\in P} \left[e^{-\frac{d_{pq}^*(t)}{R_p^0}} \right] \tag{5}$$

A_p^0 Interaction factor between pedestrian p and pedestrians q

P Set of pedestrians q perceived by pedestrian p

$d_{pq}^*(t)$ Perceived distance of pedestrian q by pedestrian p

$1/R_p^0$ Spatial discount of pedestrian p

$$\vec{o}_p(t) = -A_p^w \sum_{o\in O} \begin{bmatrix} 1 & \text{for } 0 < d_{po}^* < d_0 \\ 1 - \left(d_{po}^* - d_0\right)/d_0 & \text{for } d_0 < d_{po}^* < 2d_0 \\ 0 & \text{for } d_{po}^* > 2d_0 \end{bmatrix} \tag{6}$$

$d_{po}^*(t)$ Perceived distance of obstacle o from pedestrian p

d_o Threshold distance between pedestrian p and obstacles

A_p^w Interaction factor between pedestrian p and obstacles

Obstacles are only taken into account when these are located within a specific distance to the pedestrian. Obstacles nearby have maximum influence, while obstacles far away do not have influence. In between these distance thresholds, the repulsive force increases gradually when distance is decreasing.

The physical force $\vec{p}_p(t)$ is the force that arises when pedestrians are in contact with each other. In other terms: when the distance between their centres is equal or smaller then the sum of their radius (pedestrians are assumed to be slightly compressible). These forces are only present in high densities when collisions occur. The calibration performed in this investigation never reached such large densities and therefore its parameters were not included in the calibration. Consequently the formulations of these components are not elaborated further.

A pedestrian is only affected by pedestrians and obstacles within a limited region of the walking area (influence area). Thus P in (5) only accounts for pedestrians within this influence area. Different forms of influence areas are possible and the anisotropic shape used in the Nomad model derives from observations on pedestrian behaviour (Goffman, 1972). Pedestrians react stronger to events occurring in front of them and additionally react stronger to events closer to their axis of movement. Pedestrians are also aware of events occurring close to their back. To model this behaviour the influence area in the Nomad model consists of two elongated regions: an area in the front (larger) and an area in the back (Fig. 1.).

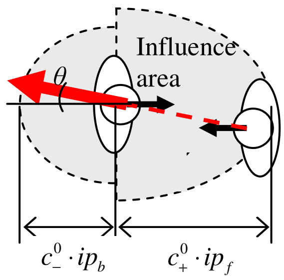

Fig 1. The Nomad influence area with the repelling force represented by the thick arrow (second term of (3))

Four parameters describing the shape of the influence area are important in the calibration presented here, namely c_+^0, ip_f, c_-^0 and ip_b. The constants c^0 controls how much the areas are elongated, if $0 < c^0 < 1$, the pedestrian is more sensitive to hindrances closer to the walking axis. The maximum distance at which another pedestrian or obstacle can be perceived in front for a c^0_+ smaller than one is $c_+^0 \cdot ip_f$ .The ip_b and c_-^0 are the equivalent for hindrances that are felt in the back.

3. LABORATORY EXPERIMENTS

The calibrations performed in this paper used data from controlled laboratory experiments conducted in the facilities of the Delft University of Technology. Various experiments have been performed to cover a wide range of pedestrian behaviours in unidirectional flows, bidirectional flows, crossing flows and in bottlenecks. The experiments have been filmed and the trajectories have been extracted via automated extraction software. A complete overview and further analyses can be found in Daamen and Hoogendoorn, 2003.

Fig 2. The narrow bottleneck experiment from Daamen and Hoogendoorn, 2003

To increase the efficiency of the calibration effort four macroscopic measures have been used. The first two choices went to the speed-density relations of the bidirectional and unidirectional flows. These are the most basic pedestrian flows and need to be correctly reproduced by any model. To improve the calibration of the bidirectional flow the distribution self organized lanes was included. The capacity of entrances is another very important aspect in pedestrian applications especially for evacuation simulations. Therefore, the capacity for a narrow bottleneck with one meter width has been used as the fourth macroscopic measure.

3.1 Fundamental diagrams from the experiments

The speed-density relations presented in Fig. 3 were derived at each time in intervals of 0.1 seconds from the derived trajectories. The speed is obtained by averaging the speed (v) of all pedestrians in the walking area and plotted against the density (k) at that time. The density is calculated dividing the amount of pedestrians by the walking area.

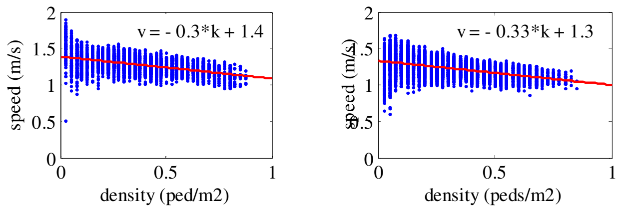

a. bidirectional flow b. unidirectional flow

Fig 3. The speed-density relations for the three flows

In Fig.3 are presented the linear regression equations for both experiments. Higher order polynomials did not improve the coefficient of determination. The variation of speeds around the regression line in the experiments (Fig.3) is due to the heterogeneity of the population. The effect of free flow speed heterogeneity is very important in pedestrian flows Campanella *et al.*, 2009. It can be observed in the speed-density graphs from the experiments that at low densities the speed variation is larger. At low densities the speed averages are closer to single pedestrians free flow speeds thus the larger variation.

3.2 Lane distribution

The lane distribution for the bidirectional flow experiment (Fig. 4) was obtained from the trajectories with an algorithm developed by Hoogendoorn *et al.*, 2008 .

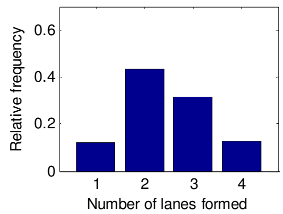

Fig 4. The frequency of lanes for the bidirectional flow

Fig 4 shows the relative frequency (count of times that a certain amount of lanes was formed / total count of times) of lanes formed. The values for the frequencies are respectively: f_1= 0.13, f_2= 0.43, f_3= 0.31 and f_4= 0.13.

3.3 Bottleneck capacity

The capacity for the narrow bottleneck experiment was estimated for the period of saturated flow. The value was obtained counting the amount of pedestrians that crossed the last section of the corridor during the period of time in which the bottleneck was saturated. These average count divided by the saturation period time in seconds resulted in 1.53 pedestrians/second.

4. CALIBRATION PROCEDURE

The calibration performed in this paper consists of comparing the relative difference of the values (*V*) of the macroscopic measures of the simulations according to (7):

$$difference = \frac{V^{sim} - V^{emp}}{V^{emp}} * 100 \quad (7)$$

The four measures generated nine values to be compared: The two coefficients of the speed-density regression (speed decay *d* and v^0) for the bidirectional and unidirectional flows (Fig.3 for the experiments), the frequencies (f_1,f_2,f_3,f_4) of the four lane amounts (Fig.4 for the experiments) and the bottleneck capacity (*c*). Both the experimental and simulated fundamental diagrams showed a large scatter causing the R^2 values of the linear regression to be around 0.2. As mentioned in the section 3.1 this mainly reflects the heterogeneity behaviour of real pedestrians. Evidently the simulations should show similar outcomes and deviations of the experimental scatter will indicate problems in the combination parameters/model. The regression coefficients are used for quantitative comparison between the simulated and experimental data. Differences between the scatter are discussed qualitatively in the following sessions.

Eight parameters from the model were chosen to be the variable criteria (4), (5) and (Table 1). These parameters are the most important affecting the interactions between pedestrians in the simulated flows. To minimise the search space 19 different sets of parameters have been generated modifying only one criteria parameter from a base parameter set (Table 1). The underlined values in the Table 1 refer to the base parameter set. For each parameter set 20 simulations have been run. All speed-density pairs obtained for each of the twenty runs were used to create the fundamental diagrams presented in the (Figs. 5, 6 and 7). For further details refer to Campanella *et al.*, 2008.

Table 1. Parameters varied in the calibration

parameter	*Values*
s^0	0, <u>0.26,</u> 0.35
T	0.1, <u>0.15</u>, 0.25, 0.5
A^0	10, <u>20</u>, 27, 30
R^0	0.1, <u>0.16</u>, 0.32
ip_f	1, <u>3</u>, 6
ip_b	0.65, <u>1</u>, 3
c_+^0	0.8, <u>0.85</u>, 0.9
c_-^0	<u>0.9</u>, 0.95, 1.05

5. RESULTS FOR THE BASIC NOMAD MODEL

The performance of the parameters sets varied significantly. One aspect was decisive for the quality of the calibration: the probability of gridlock. Gridlock is the total standstill of pedestrians obstructing each other. The probabilities varied along the sets. Six sets presented 100% of gridlocks and only four parameter sets never presented gridlocks: the base set (a.) with all underlined parameters, the set with s^0 = 0 (b.), the set with T=0.25(c.) and the set with A^0= 27 (d.). Since the densities reached by the bidirectional flow were only moderate (around 1 ped/m^2) all flows with gridlock are not further included in this paper. The Tables 2, 3 and 4 shows the results for the four parameters sets that did not present gridlocks in the simulated densities.

Table 2. Results for the speed-density regression

sets	d_{bid}	*diff*	v^0_{bid}	*Diff*	d_{uni}	*diff*	v^0_{uni}	*diff*
a.	-0.22	-26	1.35	-3	-0.07	-79	1.4	5
b.	-0.25	-15	1.44	4	-0.14	-57	1.5	9
c.	-0.32	7	1.36	-2	-0.07	-79	1.4	5
d.	-0.29	-2	1.36	-2	-0.09	-73	1.4	5

Table 3. Results for the lane distribution

sets	f_1	*diff*	f_2	*Diff*	f_3	*diff*	f_4	*diff*
a.	0.30	136	0.35	-19	0.22	-29	0.13	-2
b.	0.25	94	0.33	-23	0.35	15	0.06	-53
c.	0.25	97	0.40	-8	0.27	-13	0.08	-38
d.	0.28	117	0.32	-26	0.36	17	0.04	-70

Table 4. Results for the capacity

sets	*c*	*diff*
a.	1.8	18
b.	1.8	16
c.	1.7	7
d.	1.8	13

The results for the speed density regressions have been quite different for the bidirectional and the unidirectional flows. The former presented good fits for sets c. and d. and reasonable fits for the remaining sets. However, the four sets showed very bad fits for the unidirectional flow. All of them had a too efficient flow with an underestimated speed decay value (Table 2).

The lane distribution of all sets did not show good fits. All the flows presented too many one lanes and too little four lanes (Table 3). The capacity for all sets was over estimated with the exception of set c (Table 4).

It can be observed in the Fig. 5 that for all the sets there is a much bigger variation of speeds bellow the regression line when compared with the experiments. The sets a., c. and d. had the same value for s^0 and display larger variation of speeds. However, the set b. with $s^0 = 0$ also showed a large variation bellow the regression line. An inspection of the simulated data showed that these too low speeds occurred due to head-on collisions of pedestrians. These collisions reduced the speed of some pedestrians to almost stand still, regardless of the surrounding densities. A head-on collision occurs when two pedestrians are walking towards each other along a similar path. When this occurs the angle between the current speed and the repelling acceleration (angle θ in Fig. 1) is very small. Therefore the tendency to change the speed direction is very small, since the lever of the force is very small. The pedestrians thus continue walking towards each other until the repelling accelerations almost stop the pedestrians. At this moment any small direction difference multiplied by the very large accelerations due to the proximity finally make the pedestrians pass each other.

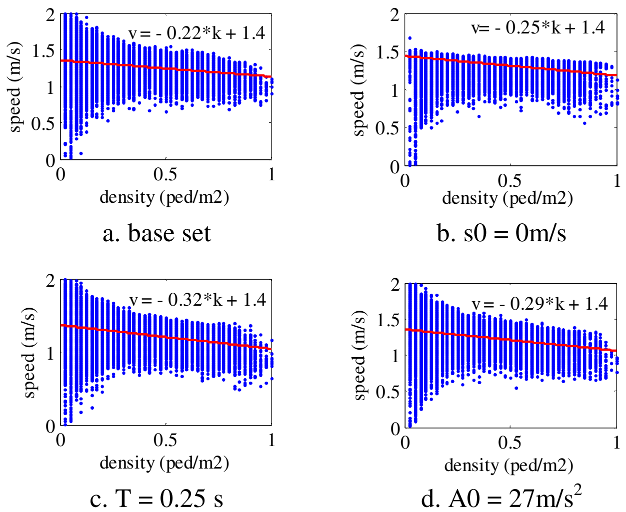

a. base set b. s0 = 0m/s

c. T = 0.25 s d. A0 = 27m/s^2

Fig 5. Speed-density relations for simulated bidirectional flows with the basic Nomad model

All sets but b. (Fig 5b.) show a large variation of speeds above the regression line. The set b. on the contrary shows a much lower variation. The increase of speeds well above the free flow speeds in the low densities is also explained by inspecting the trajectories. When two pedestrians are walking in the same direction and a faster follower pedestrian does not deviate early enough he gets very close behind the slower pedestrian. At this moment the leader feels an extra acceleration from the back due to the back side of the influence area. This acceleration occurs due to the nature of the repulsion term of (3) and the shape of the influence area (Fig.1) and not due to contact between the pedestrians. Depending on the proximity this extra acceleration pushes the pedestrian above his desired speed for some instances. This also explains why the parameter set b. does not show this upward variation since all pedestrians have the same desired speed and seldom pedestrians will walk very close behind another pedestrian. It has to be mentioned that parameter sets with very low influence from the back part of the influence area presented the highest probability to gridlock. This shows that this push from behind is being used to compensate other deficiencies in the model.

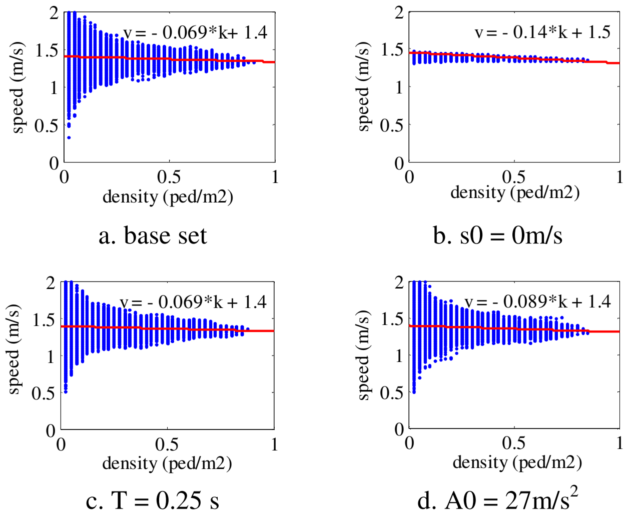

a. base set b. s0 = 0m/s

c. T = 0.25 s d. A0 = 27m/s^2

Fig 6. Speed-density relations for the simulated unidirectional flows with the basic Nomad model

The results for the unidirectional speed-density relations are shown in Fig.6. All sets present very low decay for the regression indicating that the flows are too efficient. The cause can also be attributed to the push from behind problem. This is confirmed by the results for the parameter set s0=0 (Fig.6b) were the value of the decay is twice as large as for the other sets since there is very little push from behind. Additionally sets with large c_{-}^{0} and small ip_b presented larger decays.

6. MODIFICATION OF THE NOMAD MODEL

To improve the manoeuvrability of pedestrians in opposite flows, the pedestrian repulsion term $\vec{r}_p(t)$ (5) is modified by adding the extra repulsion defined by (8).

$$\vec{a}_p^{\,front-}(t) = -A_p^- \sum_{q \in P_{front}^-} e^{-\frac{d_{pq}^*(t) * d_{pq}^{y*}(t)}{R_p^-}} \tag{8}$$

Where:

P_{front}^- Set of pedestrians perceived by pedestrian p walking in the front part of the influence area and in opposing direction

A_p^- Interaction factor for opposing pedestrians

$d_{pq}^{y*}(t)$ Perceived lateral distance from pedestrian p towards pedestrian q

$1/R_p^-$ Spatial discount of pedestrian p for opposing pedestrians

This extra term accentuates the repulsion acceleration arisen by lateral distances $d_{pq}^{y*}(t)$ from pedestrians walking in the opposite directions. The lateral distance is the distance the pedestrian q is from the walking axis of pedestrian p (Fig. 7).

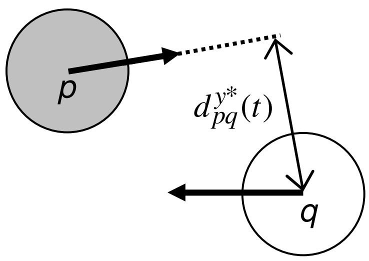

Fig 7. Perceived lateral displacement of pedestrian q

The other modification is a limited form of anticipation (9) that displaces the perceived position (x, y) of pedestrians in the direction of their speed (v_x, v_y).

$$\begin{aligned} x' &= x + v_x \Delta_a \\ y' &= y + v_y \Delta_a \end{aligned} \tag{9}$$

Δ_a Anticipation time

The displaced position (x', y') is applied only on opposing pedestrians and pedestrian p itself. This anticipation decreases the perceived distances proportionally to the speeds of opposing pedestrians. Smaller lateral distances increase the lateral acceleration pushing the trajectories away from each other. The value of the anticipation time used is 0.5s.

7. RESULTS OF THE MODIFIED NOMAD MODEL

The modifications presented in the previous section have been implemented and new simulations for the 19 sets have been run. The manoeuvrability of pedestrians is improved and is indicated by the reduction of the probability of grid locking for most sets. The parameter set ip_b = 0.65 (e) with smaller back part of the influence area delivered the best results.

Table 5. Results for the speed-density regression

sets	d_{bid}	*diff*	v^0_{bid}	*diff*	d_{uni}	*diff*	v^0_{uni}	*diff*
e.	-0.28	-7	1.40	1	-0.25	-24	1.40	5

Table 6. Results for the lane distribution

sets	f_1	*diff*	f_2	*diff*	f_3	*diff*	f_4	*diff*
e.	0.34	163	0.38	-12	0.28	-11	0.01	-92

Table 7. Results for the capacity

sets	*c*	*diff*
e.	1.6	4

The speed-density regression values for the unidirectional flow presented much better fit (Table 5). The speed variation along the densities for the bidirectional flow diminished. Additionally, the capacity of the bottleneck showed good fit. However, the speed variability in the lower densities for both bidirectional and unidirectional flows (Figs.8a and 8b) is still too high.

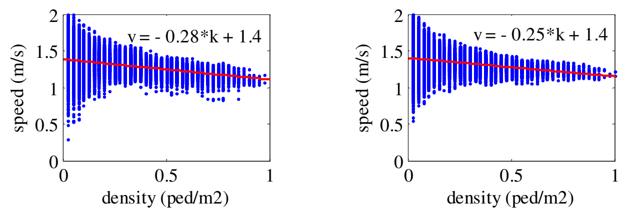

a. bidirectional flow b. unidirectional flow

Fig 8. Speed-density relations for the modified Nomad model

The overall lane distribution (Table 6.) did not present a good result with the same over-estimation of one lane frequency and under-estimation of four lanes. These discrepancies were exacerbated in the new model. Inspecting the trajectories revealed that the improved capacity of avoiding head-on collisions had the side effect of increasing the probability of a pedestrian joining an existing lane instead of creating new ones. Pedestrians with a larger push from behind (so as in the basic model) are able to create more stable lanes by having their acceleration more aligned to the corridor direction.

These observations may have an important implication for the quality of the model.

8. CONCLUSIONS

This investigation presented a detailed data analysis of pedestrian simulation flows. Two problems with the basic Nomad model were identified: an excessive "push from behind" and "head-on" collisions. A solution for both was implemented and showed to improve the quality of the predictions.

The Nomad model was effectively calibrated for four important measures of pedestrian flows: speed-density relations for bidirectional and unidirectional flows and the capacity of narrow bottlenecks. These results show that a microscopic model can be generalised predicting correctly different types of flows. However, the problems with the distribution of lanes described in the Section 7 indicate that the modified model may still not be properly calibrated for all types of flows.

The second calibration effort after the basic Nomad model has been modified delivered better results when compared with the basic model. This indicates that the trajectory analysis performed in the Section 5 was effective in revealing the causes of bad fits. The necessity of recurring to trajectories to understand the shortcomings of calibrations suggests that a microscopic approach to calibration may be more effective in delivering generalized microscopic models.

Future research will incorporate flows with higher densities in the calibration process. The flows investigated in this paper presented only low and moderate densities. The narrow bottleneck experiment presented moderate to high densities but only the capacity was used for the calibration. Furthermore, crossing flows should also be investigated to increase the applicability of the model.

REFERENCES

Asano, M., Kuwahara, M. and Tanaka, S. (2007). Multi-directional pedestrian flow model based on empirical data. *11th World Conference on Transportation Research.* 11 ed. Berkely, USA.

Berrou, J. L., Beecham, J., Quaglia, P., Kagarlis, M. A. and Gerodimos, A. (2005). Calibration and validation of the Legion simulation model using empirical data. *Pedestrian and Evacuation Dynamics.* Springer-Verlag**,** 167-181.

Brockfeld, E., Kühne, R. D. and Wagner, P. (2004). Calibration and Validation of Microscopic Traffic Flow Models. *Transportation Research Record,* 1876**,** 62-70.

Buchmueller, S. and Weidmann, U. (2006). Parameters of pedestrians, pedestrian traffic and walking facilities. *Ivt Report no.132.* Zürich, ETH

Campanella, M., Hoogendoorn, S. and Daamen, W. (2008). Calibration of pedestrian models with respect to self-organisation. *TRAIL congress 2008.* Delft, TRAIL Research School.

Campanella, M., Hoogendoorn, S. and Daamen, W. (2009). Effects of Heterogeneity in Self-Organized Pedestrian Flows. *to appear in Transportation Research Record (TRR).*

Daamen, W. and Hoogendoorn, S. (2003). Controlled experiments to derive walking behaviour. *European Journal of Transport and Infrastructure Research* 3**,** 39-59.

Goffman, E. (1972). *The Individual as a Unit. Relations in Public: Microstudies of the Public Order.* Allen Lane The Penguin Press, London.

Helbing, D., Buzna, L., Johansson, A. and Werner, T. (2005). Self-Organized Pedestrian Crowd Dynamics: Experiments, Simulations, and Design Solutions. *Transportation Science,* 39**,** 1-24.

Hoogendoorn, S. and Bovy, P. H. L. (2003). Simulation of pedestrian flows by optimal control and differential games. *Optim. Control Appl. Meth.,* 24**,** 153–172.

Hoogendoorn, S. and Daamen, W. (2005). Self-Organization in Pedestrian Flow. *Traffic and Granular Flow '03.* 373-382.

Hoogendoorn, S., Daamen, W. and Campanella, M. (2008). Self-organization and Chaos in Pedestrian Flow: Experiments and modelling. *Proceedings of the Chaotic Modeling and Simulation International Conference.* Chania, Crete.

Hoogendoorn, S., Daamen, W. and Landman, R. L. (2005). Microscopic calibration and validation of pedestrian models: cross-comparison of models using experimental data. IN WALDAU, N.*, et al.* (Eds.) *Pedestrian and Evacuation Dynamics.* Springer-Verlag**,** 253-265.

Klüpfel, H. (2005). The simulation of crowd dynamics at very large events–Calibration, empirical data, and validation. IN WALDAU, N.*, et al.* (Eds.) *Pedestrian and Evacuation Dynamics.* Springer-Verlag**,** 285-296.

Pelechano, N., Allbeck, J. M. and Badle, N. I. (2007). Controlling Individual Agents in High-Density Crowd Simuation. *ACM SIGGRAPH / Eurographics Symposium on Computer Animation (SCA'07)* San Diego (USA).

Seyfried, A. and Schadschneider, A. (2008). Fundamental Diagram and Validation of Crowd Models. *Proceedings of the 8th international conference on Cellular Automata for Reseach and Industry.* Yokohama, Japan, Springer-Verlag.

Teknomo, K. (2006). Application of microscopic pedestrian simulation model. *Transportation Research Part F: Psychology and Behaviour,* 9**,** 15-27.